THE AMERICAN MINERALOGIST, VOL. 56, MAY-JUNE, 1971

# VIBRATIONAL SPECTRA OF HIGH-CALCIUM PYROXENES AND PYROXENOIDS

MARTIN S. RUTSTEIN[1]
*Department of Geology, Juniata College, Huntingdon, Pa. 16652*

AND

WILLIAM B. WHITE[2]
*Materials Research Laboratory, The Pennsylvania State University, University Park, Pa. 16802*

ABSTRACT

IR and optical spectra have been measured on hydrothermally synthesized pyroxenes with compositions along the joins connecting the compositions $CaSiO_3$, $MnSiO_3$, $CaMgSi_2O_6$, $CaMnSi_2O_6$, and $CaFeSi_2O_6$. The objectives were to compare changes in the spectra with structural changes. The optical spectra are due to ferrous iron and appear insensitive to structural detail. The infrared spectra, particularly the Si-O stretching vibrations, vary markedly with small structural changes. Each structure type, diopside, wollastonite, bustamite and rhodonite has a distinct *ir* spectrum. Spectral changes with composition are small. Two phase mixtures can be distinguished. IR evidence indicates that the high-temperature form of hedenbergite has the bustamite rather than the wollastonite structure.

## INTRODUCTION

Infrared spectra of various pyroxenes have been published by numerous authors including Launer (1962), Lazarev and Tenisheva (1961a and 1961b), and Lyon (1967). Mostly these have been concerned with a comparison of the chain silicates with other silicate structures or of the main pyroxene families with each other. It has been recognized that the IR spectra of pyroxenes show distinct differences from one mineral to another but these do not seem to have been closely examined.

This paper is concerned with the high calcium apex of the $CaSiO_3$–$MgSiO_3$–$FeSiO_3$–$MnSiO_3$ tetrahedron. Compounds have been synthesized along the diopside-hedenbergite-bustamite triangle and along the tetrahedral edges connecting this triangle with the wollastonite apex. Our objective is to follow the changes in composition by infrared spectroscopy and to compare the spectral changes with structural changes.

## EXPERIMENTAL METHODS

*Phase Synthesis.* Starting materials were reagent grade $CaCO_3$, MgO, $Fe_2O_3$, $MnO_2$, and silicic acid ($SiO_2 \cdot XH_2O$) which were carefully dehydrated before weighing. These materials in the desired proportions were mixed for three hours in a mechanical shaker, fired in

[1] Present address: Department of Geology, State University of New York At New Paltz, New Paltz, New York.

[2] Also affiliated with the Department of Geochemistry and Mineralogy.

air at approximately 925° – 950°C for fifteen minutes in a silver foil-lined silica glass boat, and hand-ground under acetone in a synthetic sapphire mortar for approximately one hour. Compositions along the joins $CaMgSi_2O_6$-$CaMnSi_2O_6$, $CaSiO_3$-$MnSiO_3$, and $CaSiO_3$-$CaFeSi_2O_6$ were prepared in this manner. Compositions along the join $CaMgSi_2O_6$-$CaFeSi_2O_6$ were also prepared and were favorably compared to previously prepared similar compositions (Rutstein and Yund, 1969) to insure the reproducibility of method and technique.

Synthesis was carried out using standard hydrothermal techniques in Tuttle-type cold-seal pressure vessels, using the oxygen buffer technique of Eugster and Wones (1962). The QFM buffer was employed for all iron-bearing runs and some manganese-bearing runs. The majority of the manganese-bearing runs (without iron) were buffered by the pressure vessel (approximately NNO according to Eugster and Wones, 1962). The charges were placed in $Ag_{70}$ $Pd_{30}$ tubing. For (Ca, Fe)$SiO_3$ compositions the temperature of synthesis was 850°–995°C; for (Ca, Mn)$SiO_3$ compositions this was 750°C; for Ca(Mg, Fe)$Si_2O_6$ compositions, this was 750°C; and for Ca(Mg, Mn, Fe)$Si_2O_6$ compositions, this was 450°–550°C. All runs were made at 1 kb water pressure. Run duration was generally from seven to fourteen days for the higher temperatures and two to five weeks for the lower temperatures. Runs were quenched with an air blast. Only runs that showed negligible weight change, maintenance of the buffer at the conclusion of the run, and at least 98 weight per cent yield of pyroxene *or* pyroxenoid (traces of $SiO_2$ and $Mn_3O_4$ were observed) were considered successful.

The run products were studied using standard oil immersion and X-ray techniques. Samples were examined using a Tem-Pres diffractometer with CuK$\alpha$ radiation. Rapid and sure distinction between pyroxenes and pyroxenoids was made possible by examination of reflections in the interval 24°–36° $2\theta$. Details of X-ray characterization will be presented elsewhere.

*Spectral Measurements.* Specimens for infrared measurement were prepared by grinding 1 mg of sample with 300 mg of KBr and cold-pressing the material under vacuum into a transparent disc. Spectra of these discs were obtained over the range of 4000 to 250 $cm^{-1}$ on a Perkin-Elmer Model 621 spectrophotometer. No difficulties were encountered with the spectral measurements.

Optical spectra were obtained from powders by diffuse reflectance spectroscopy. The powdered mineral was packed into a shallow aluminum holder. Light reflected from the powder surface was measured on a Beckman DK-2A spectrophotometer using a Kodak $BaSO_4$ paint in the reference beam. Background was determined using $CaSiO_3$ and $CaMgSi_2O_6$ standards. It should be noted that diffuse reflectance measurements yield an absorption spectrum directly; no mathematical transformations are necessary.

## Theoretical Analyses

A factor group analysis was performed on the diopside structure to determine the number of expected infrared bands. The mathematical techniques are discussed in an earlier paper (White and DeAngelis, 1967).

Table 1 shows the invariance conditions for the diopside structure. Space group $C2/c$ contains the $C_{2h}$ factor group. Only the cations lie on elements of symmetry and are thus restricted in their vibrational motion. The invariance conditions yield a reducible character which contains the symmetry properties of the vibrational degrees of freedom of the entire unit cell. The reducible representation is decomposed into the irreducible representations of $C_{2h}$ in the Table 2. The factor group has a center of

TABLE 1. INVARIANCE CONDITIONS FOR DIOPSIDE

| $C_{2h}$ | $E$ | $C_2$ | $i$ | $\sigma_h$ |
|---|---|---|---|---|
| $8(f)$ $C_1$ | $E$ | — | — | — |
| 24 $O^{-2}$+8 $Si^{4+}$ | 32 | 0 | 0 | 0 |
| $4(e)$ $C_2$ | $E$ | $C_2$ | — | — |
| 4 $Ca^{2+}$+4 $Mg^{2+}$ | 8 | 8 | 0 | 0 |
| $\omega_p$ | 40 | 8 | 0 | 0 |
| $\chi$ (cell) | 120 | −8 | 0 | 0 |
| $\chi$ (prim) | 60 | −4 | 0 | 0 |

symmetry and this breaks the vibrations into sets which vibrate symmetrically to the center and sets which vibrate antisymmetrically to it. The second column gives the total number of vibrations in each symmetry species. Out of these we can separate the internal vibrations of the two-tetrahedron links of the pyroxene chains. Since both silicon and oxygen are on general positions, these degrees of freedom distribute uniformly among the symmetry species with 9 vibrations in each. Structures of lower symmetry such as that of wollastonite or bustamite yield even less information. About the only conclusion to be drawn from this analysis is that there should be a total of 18 infrared active bands due to motions of the chain. Perhaps half of these will be of stretching character. The spectra were obtained on powders so both polarization directions are superimposed and will probably overlap. Thus there are perhaps 4 to 9 bands expected in the Si–O stretching region and this is, of course, what is observed. It does show that a great deal of information is not missing except for the polarization dependence. Polarized spectra from single crystals could double the number of observable modes.

## OPTICAL SPECTRA

The optical spectra of the iron-containing compositions are given in Figure 1. The high temperature hedenbergite spectrum is characteristic

TABLE 2. NORMAL MODES AND SELECTION RULES

| $C_{2h}$ | Total Modes | Acoustic | Chain Vibrations | Lattice Vibrations | Selection Rules |
|---|---|---|---|---|---|
| $A_g$ | 14 | | 9 | 5 | Raman |
| $B_g$ | 16 | | 9 | 7 | Raman |
| $A_u$ | 14 | 1 | 9 | 4 | IR, $E \parallel b$ |
| $B_u$ | 16 | 2 | 9 | 5 | IR $E \perp b$ |

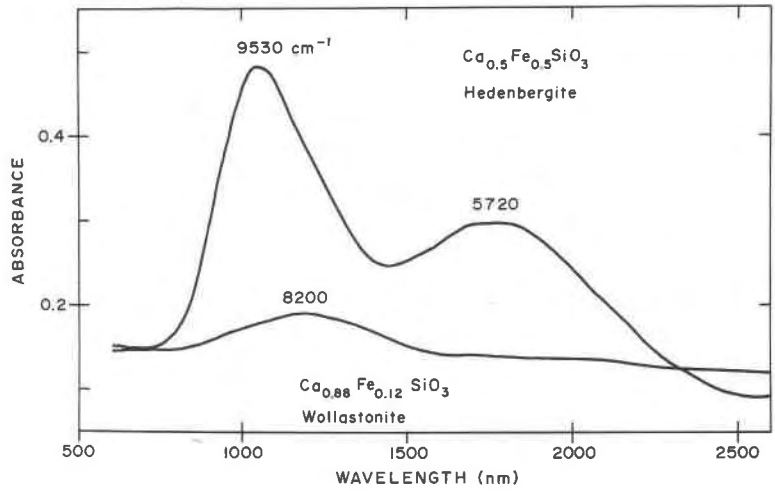


FIG. 1. Optical spectra of high temperature hedenbergite and iron-rich wollastonite.

of the diopside type structure (White and Keester, 1966) and is quite distinct from the wollasonite structure shown below. However, the bands do not shift much as a function of composition and do not yield much information.

## INFRARED SPECTRA

*Comparison of End Members.* The interpretation of the infrared spectra can be started with the spectrum of diopside shown in Figure 2. It has a very characteristic pattern with three strong bands in the range of 1050 to 850 $cm^{-1}$. This basic pattern can be designated the "diopside" type. The 5 modes at high frequencies are representative of stretching motions in the silicate chain. In comparison, the spectra of hedenbergite (Fig. 2) and johannsonite (Fig. 2) are very similar. One weak sharp band in diopside moves to lower frequencies as iron or manganese is added and becomes a shoulder of the lowest frequency band in both hedenbergite and johannsonite. The others remain nearly constant which suggests that the chain vibrations are not particularly sensitive to the population of the cation sites.

The spectrum of wollasonite is shown in Figure 3. There are two distinctive clusters of three bands each in the high-frequency region.

The spectrum of bustamite (Fig. 3) is the third distinctive pattern. The high-frequency group consists of two sets of two bands each. The basic pattern changes little with changing composition providing that no structural change takes place. The comparison with the spectrum of

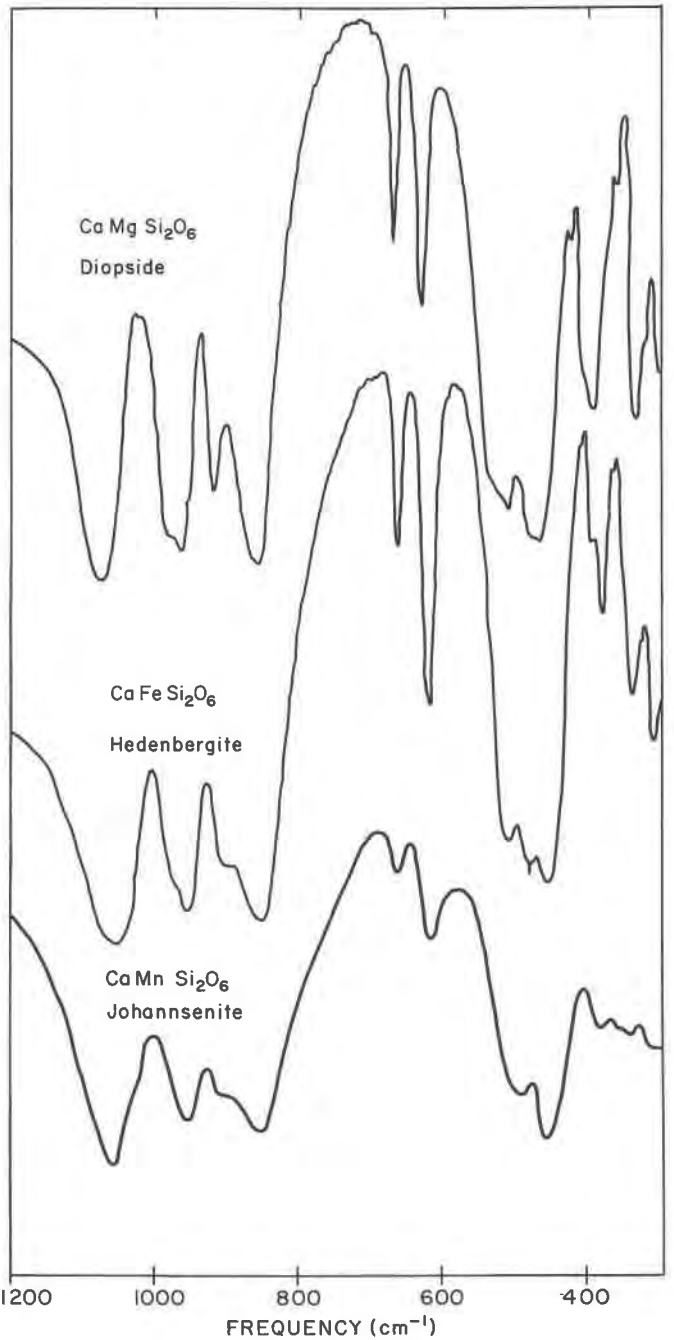


FIG. 2. IR spectra of diopside structure pyroxenes. Johansenite was natural specimen from Italy. All others were synthetics.

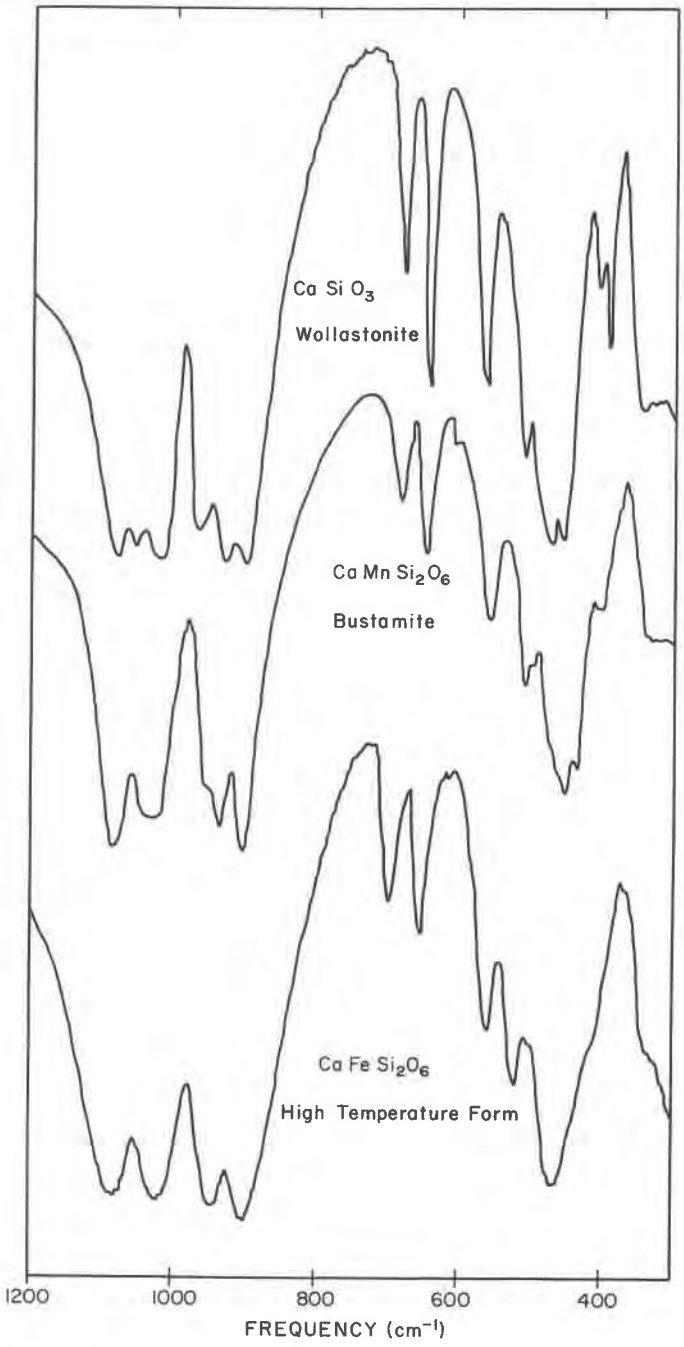


FIG. 3. IR spectra of wollastonite and bustamite structure pyroxenoids.

the high-temperature form of $CaFeSi_2O_6$ is interesting (Fig. 3). The spectrum is very similar to that of bustamite but is unlike that of wollastonite. The structure of high-temperature $CaFeSi_2O_6$ has long been considered to be a wollastonite solid solution (Bowen *et al.*, 1933) as was formerly the case for bustamite. Peacor and Prewitt (1963) showed that bustamite has a structure distinct from that of wollastonite with space group $A2/m$ instead of $P2_1/m$ of wollastonite. The difference lies in the relative arrangement of the chains and this should manifest itself in the infrared spectrum. Based on the comparison in Figure 3, we suggest that the high-temperature $CaFeSi_2O_6$ also has the $A2/m$ bustamite structure.

Attention should be called to the sharp weak bands near 700 $cm^{-1}$. Lazarev and Tenisheva (1961a) and later Ryall and Threadgold (1966) proposed that the number of these bands was determined by the number of tetrahedra in the chain repeat unit. This number would be 2 for pyroxenes and 3 for the pyroxenoids. The results of these spectra substantiate these conclusions. A detailed comparison of these spectra is shown in Figure 4. Because of their sharpness, these bands are useful for recognizing two-phase mixtures.

*The Diopside Solid Solutions.* Between diopside and hedenbergite is a complete solid solution with no evidence for phase separation or structural change (Rutstein and Yund, 1969). The infrared spectra reflect this and only minor shifts in band frequencies are observed. The characteristic diopside pattern is retained at all intermediate compositions.

Along the join between diopside and $CaMnSi_2O_6$ and between hedenbergite and $CaMnSi_2O_6$ changes occur because of the formation of the bustamite phase. Due to kinetic problems, johannsonite could not be synthesized pure under any conditions used. At 750°C, the infrared spectra show the characteristic pattern of the diopside structure out to $CaMg_{0.7}Mn_{0.3}Si_2O_6$. At the manganese-rich end, the characteristic bustamite pattern is observed from $CaMnSi_2O_6$ to $CaMg_{0.2}Mn_{0.8}Si_2O_6$. Intermediate compositions appear to be a mixture of the two. This is confirmed by X-ray and microscopic examination.

Along the hedenbergite to $CaMnSi_2O_6$ join, the characteristic pattern of the diopside structure persists at least to $CaFe_{0.5}Mn_{0.5}Si_2O_6$ with a two-phase region between this composition and $CaFe_{0.2}Mn_{0.8}Si_2O_6$ at 750°C. In general, the two-phase regions determined by infrared spectra and the two-phase regions observed by X-ray techniques were in agreement.

*The Wollastonite Solid Solutions.* As manganese is added to wollastonite, the characteristic wollastonite pattern remains intact to about $Ca_{0.75}Mn_{0.25}SiO_3$ and then changes over a very narrow composition range to

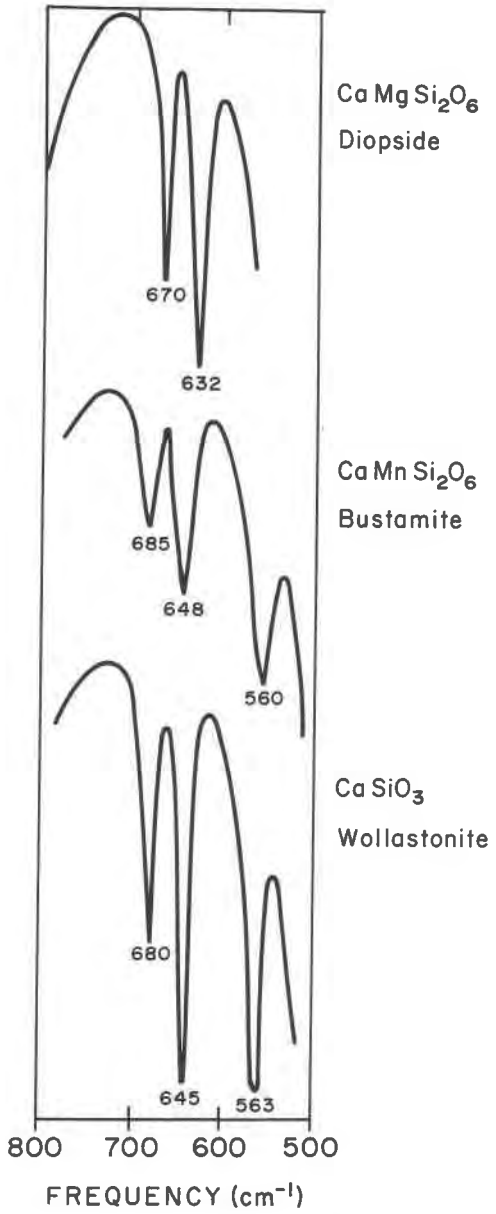


FIG. 4. Comparison of 700 $cm^{-1}$ region for pyroxene and pyroxenoid spectra.

the characteristic bustamite pattern. It is here emphasized again that the frequencies of these groups of bands change very little with composition (quite unlike the infrared spectra of most solid solutions) and instead the patterns shift abruptly at phase boundaries. The bustamite pattern remains throughout the composition range down to $Ca_{0.10}Mn_{0.90}$ where the rhodonite pattern appears.

The rhodonite pattern is defined for the $MnSiO_3$ end member in Figure 5. The spectrum is more complex, presumably because of the 5 tetrahedron repeat unit. The 700 $cm^{-1}$ region contains 5 sharp bands as expected for the fünferketten structure. The $MnSiO_3$ end member, prepared at 750°C, shows all of the complexity that might be expected from the longer chain repeat length. The $Ca_{0.1}Mn_{0.9}SiO_3$ composition yields a spectrum with less resolved detail and by $Ca_{0.2}Mn_{0.8}SiO_3$ [the "ideal" rhodonite composition according to Peacor and Niizeki (1963)] the pattern is very close to that of bustamite. $Ca_{0.7}Mn_{0.3}SiO_3$ has an unperturbed bustamite spectrum. These results are in good agreement with the data of Glasser (1962) who found the upper stability limit of rhodonite at 10 mole percent $CaSiO_3$ in the temperature range of 1000 to 1200°C.

As iron is added to $CaSiO_3$ at 850°C, the characteristic wollastonite pattern persists to $Ca_{0.88}Fe_{0.12}SiO_3$. Then, over a composition range of no more than a few percent, the wollastonite pattern gives way to the bustamite pattern. Solid solutions more rich in iron then retain the same bustamite-like infrared spectrum down to the $CaFeSi_2O_6$ composition. This abrupt change in the infrared spectrum lends credibility to the hypothesis proposed earlier that the high-temperature form of $CaFeSi_2O_6$ is a bustamite-like structure and is distinct from wollastonite. Wollastonite, it appears, will accept only limited amounts of either iron or manganese in solid solution before cation ordering takes place.

A summary of the composition limits of various structures encountered in the infrared spectra is given in Figure 6.

Acknowledgment

This research was supported by the Pennsylvania Science and Engineering Foundation under a cooperative agreement between The Pennsylvania State University and Juniata College. We are grateful to Juniata undergraduates Jeffery Albright and Susan Shaler for collecting much of the experimental data.

References

Bowen, N. L., J. F. Schairer, and E. Posnjak (1933) The system CaO-FeO-$SiO_2$. *Amer. J. Sci.* **26,** 193–284.

Eugster, H. P., and David R. Wones (1962) Stability relations of the ferruginous biotite, annite. *J. Petrology* **3,** 82–125.

Glasser, F. P. (1962) The ternary system CaO-MnO-$SiO_2$. *J. Amer. Ceram. Soc.* **45,** 242–249.

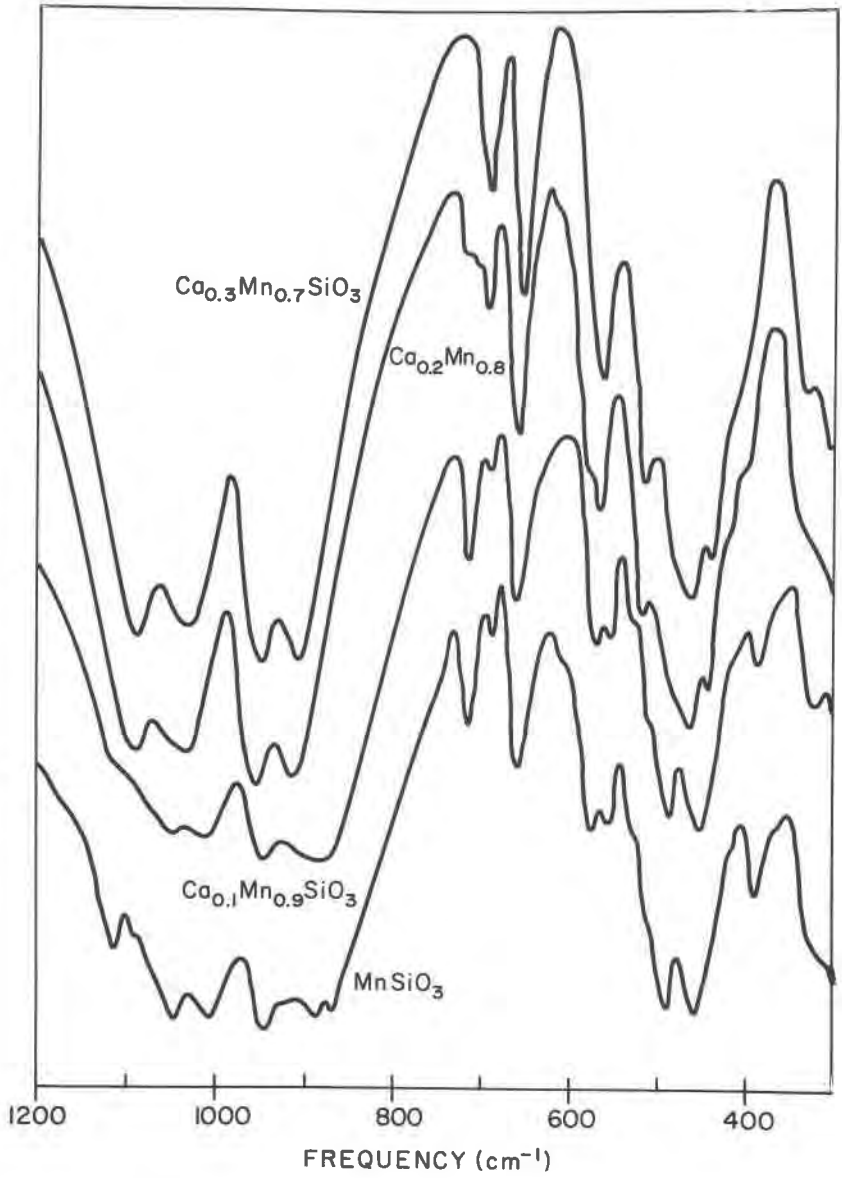


FIG. 5. IR spectra of various compositions near $MnSiO_3$.

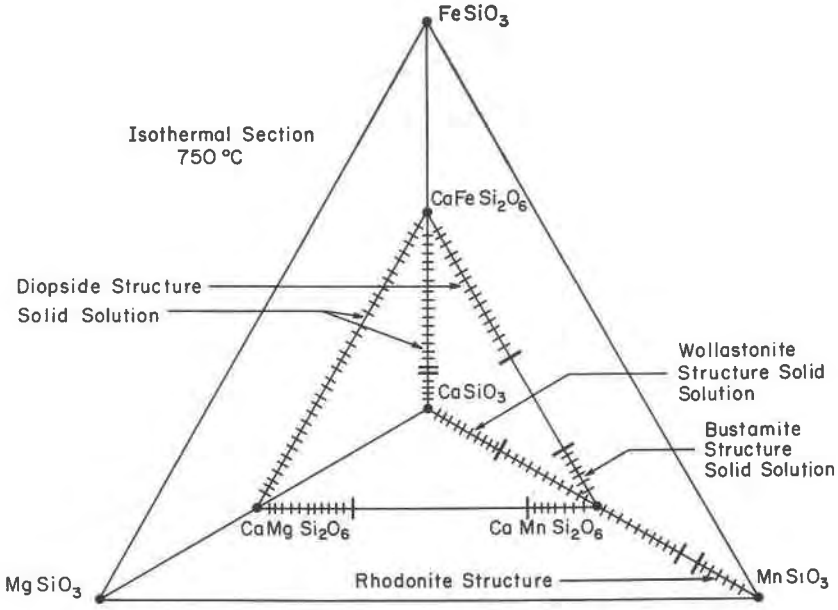


FIG. 6. Solid solution and phase boundaries found by ir spectroscopy, in the system $CaSiO_3$-$MgSiO_3$-$MnSiO_3$-$FeSiO_3$.

LAUNER, P. J. (1952) Regularities in the infrared absorption spectra of silicate minerals. *Amer. Mineral.* **37,** 764–784.

LAZAREV, A. N., AND T. F. TENISHEVA (1961a) The vibrational spectra of silicates II. Infrared absorption spectra of silicates and germanates with chain anions. *Opt. Spektrosk.* **10,** 79–85 [*Opt. Spectrosc.* **10,** 37–40].

——— (1961b) Vibrational spectra of silicates III. Infrared spectra of pyroxenoids and other chain metasilicates. *Opt. Spektrosk.* **11,** 584–587 [*Opt. Spectrosc.* **11,** 316–317].

LYON, R. J. P. (1967) Infrared absorption spectroscopy, In J. Zussman (ed.) *Physical Methods in Determinative Mineralogy.* Academic Press, London, 371–403.

PEACOR, DONALD R. AND NOBUKAZU NIIZEKI (1963) The redetermination and refinement of the crystal structure of rhodonite, (Mn, Ca)$SiO_3$. *Z. Kristallogr.* **119,** 98–116.

———., AND C. T. PREWITT (1963) Comparison of the crystal structures of bustamite and wollastonite. *Amer. Mineral.* **48,** 588–596.

RUTSTEIN, MARTIN S., AND RICHARD A. YUND (1969) Unit-cell parameters of synthetic diopside-hedenbergite solid solutions. *Amer. Mineral.* **54,** 238–245.

RYALL, WILLIAM R., AND IAN M. THREADGOLD (1966) Evidence for, $SiO_3)_5]\alpha$ type chains in inesite as shown by X-ray and infrared absorption studies. *Amer. Mineral.* **51,** 754–761.

WHITE, W. B., AND B. A. DEANGELIS (1967) Interpretation of the vibrational Spectra of spinels. *Spectrochim. Acta* **23A,** 985–995.

———, AND K. L. KEESTER (1966) Optical absorbtion spectra of iron in the rock-forming silicates. *Amer. Mineral.* **51,** 774–791.

*Manuscript received, September 21, 1970; accepted for publication, October 22, 1970.*